European Journal of Clinical Pharmacy
Print ISSN: 2385-409X **Online ISSN**: 3105-0409
Website: https://farmclin.com/

Original Research Article

The added value of Multidetector Computed Tomography Cardiac Angiography in the Diagnosis of Congenital Cardiovascular Anomalies

Article History:

Name of Author:
Omran K.Q[1], Hany M. A[2], Hazem A.Y[3], Sara A.G[4] and Wesam I. E[5]*

Affiliation:

Corresponding Author:
Sara Ali Gamal

Received: 09-07-2025
Revised: 22-07-2025
Accepted: 06-08-2025
Published: 27-08-2025

Abstract: ***Introduction***: Transthoracic echocardiography (TTE) is the primary noninvasive imaging technique for evaluating congenital heart diseases (CHD). Similarly, computed tomography angiography (CTA) offers a valuable means of examining cardiac anomalies and extracardiac structures. ***Objectives:*** This study aimed to evaluate the role of CTA in diagnosing CHD and to compare the diagnostic accuracy of TTE and CTA. ***Methods:*** A total of 112 patients underwent preoperative evaluation with TTE and CTA using a 128-multidetector scanner with retrospective ECG gating. The imaging was analyzed using a segmental approach, focusing on three primary CHD types: cardiac malformations, anomalies of the heart-great vessel connections, and congenital vascular anomalies. For a more detailed analysis, these categories were further divided into subgroups based on surgical characteristics. The diagnostic accuracy, sensitivity, and specificity of both imaging modalities were compared, with surgical or catheterization findings serving as the gold standard. ***Results:*** Patients' mean age was 9.2 ± 7.1 months. The total number of anomalies was 458; out of them were 207 intracardiac malformations, 76 heart-great vessel connection malformations, and 175 congenital vascular anomalies. Multidetector Computed Tomography (MDCT) outperformed TTE in assessing vascular and valvular anomalies, as well as pulmonary lesions. However, ECHO demonstrated greater effectiveness in evaluating cardiac malformations, while both methods showed comparable accuracy in concordance and valvular atresia. The diagnostic accuracies of MDCT were 98%, 99%, and 100% for cardiac malformations, heart-great vessel connection malformations, and congenital vascular anomalies, respectively, compared to Echo, which achieved 99%, 95% and 93% in the same categories. ***Conclusion***: The combination of MDCT and TTE has enhanced diagnostic accuracy in CHD cases, particularly for extracardiac anatomical structures, thereby reducing the necessity for cardiac catheterization, especially in critically ill patients.

Keywords: Congenital heart disease; MDCT; Transthoracic echocardiography.

INTRODUCTION

Congenital heart diseases (CHDs) are recognized as the most prevalent congenital birth defects, affecting 1% of live births (Madsen et al., (1). Despite being operator-dependent, echocardiography remains the primary noninvasive imaging technique for diagnosing and monitoring CHD in most patients (Khatri et al., (2). Although traditional angiography is considered the gold standard for CHD diagnosis, it has notable restrictions: it is invasive, requires general anesthesia, and exposes newborns to radiation and contrast agents (Rao, (3). In contrast, cardiac CT scan interpretation closely resembles that of echocardiography but does not rely on the acoustic window or operator expertise, as is the case with ultrasonography. Furthermore, cardiac CTA provides hemodynamic insights, allows for comprehensive assessment of cardiovascular and respiratory structures, and clearly defines airway and vascular anatomy. This capability enables the evaluation of extracardiac great vessels along their

full length, enhancing CTA's utility in pediatric CHD cases (Paul et al., (4). Despite its lower temporal resolution compared to echocardiography, cardiac CTA combines rapid image acquisition, expanded anatomical coverage, high three-dimensional resolution, and multiplanar reformation, along with ECG synchronization. These advancements have significantly enhanced image quality, reduced patient risks, and established MDCT as an optimal noninvasive imaging modality for evaluating pediatric patients (Orly et al., (5). With recent advancements in MR and CT technologies, cardiac catheterization is no longer crucial for diagnostic purposes (Hellinger et al., (6).

This study aimed to evaluate the role of MSCT as compared to TTE in children with congenital heart diseases, with a particular focus on thoracic congenital vascular anomalies, and to compare the diagnostic accuracy of ECHO and CTA.

Patients and Methods

Ethical considerations:

The protocol and informed consent forms used in this study were approved by Assiut University Hospital. Written informed consent was obtained from all parents before any procedure.

Patients:

Our study included 112 patients with CHD or vascular anomalies. It was conducted from June 2021 to May 2023 in the MDCT unit of the radiology department at Assiut University Hospitals. There were 60 females and 52 males.

Inclusion criteria: We included pediatric patients with CHD who were diagnosed by ECHO and clinical examination and in need of further confirmation by MDCT before surgical management.

Exclusion criteria included patients with a history of hypersensitivity to iodinated contrast agents, impaired renal function, respiratory distress, fever, or arrhythmia.

Methods:

All patients underwent 128 multidetector CT scanner with retrospective ECG-gating following the completion of patient preparation, as outlined below:

a) Patient preparation:

Prior to the examination, patients were instructed to fast for 4–6 hours in consultation with the referring physician. An intravenous (IV) line was placed in a vein in the upper limb. The anesthesiologist oversaw patient sedation and monitoring, using either inhalational or oral anesthesia, with the sedation protocol tailored to the patient's age.

b) Technique of examination.

I) Non-ionic contrast media was administered (1–1.5 mL/kg) and diluted with normal saline in a 1:1 ratio to minimize streak artifacts. The injection was delivered through the IV line at a flow rate of 1.5–2 mL/s using an automatic pump. Subsequently, 20–30 mL of 0.9% saline was injected at the same rate.

Image acquisition

A. Scan protocol and parameters: The patient was positioned supine and headfirst on a 128 multidetector CT scanner. For older children, the contrast-enhanced ECG-gated scan was completed in a single breath-hold. The bolus tracking technique was employed, using a region of interest placed in the proximal descending aorta or left ventricle, with a pre-defined threshold of 100–150 HU. ECG data were recorded throughout the scan. The field of view extended from the root of the neck, encompassing the proximal portions of the common carotid and subclavian arteries, to the portal vein level inferiorly. This range was critical for detecting anomalies, including aortic arch branch abnormalities, situs inversus, situs ambiguous, abdominal aortic coarctation, and infra-diaphragmatic TAPVR.

B. CT scan dose parameters: Radiation dose parameters were customized based on the patient's body build, utilizing dose-saving strategies to minimize exposure to radiation. Parameters included a tube current of 50–100 mA (adjusted by body weight at 10 mA/kg), 80–100 kV, 0.28-second rotation time, 0.48 pitch, and 0.7 mm slice thickness. Functional assessment was excluded due to the lack of suitable software for accurate ventricular function evaluation, a task that echocardiography can perform effectively in all cases.

C. A multi-phase examination of the heart was conducted, capturing sequential images during the mid-venous and mid-arterial enhancement phases to ensure complete opacification of both heart chambers and all extracardiac vessels. In cases of complex venous anomalies, a delayed phase scan (30–60 seconds post-injection) was performed, depending on the patient's age, size, and heart rate.

D. Post-Procedural Assessment: Axial images were reconstructed with a slice thickness of 1.0 mm and a 0.6 mm increment, then reviewed to ensure adequate quality. Patients were monitored for 15–30 minutes after the procedure until they fully recovered from sedation.

E. Axial images captured at different points in the cardiac cycle were reconstructed with a 0.6 mm slice thickness and analyzed using an advanced workstation. A systematic review was conducted to evaluate intra-cardiac structures, extracardiac vessels, and other thoracic anatomy.

Additional reconstruction techniques included:

Three-Dimensional Volume Rendering (3D-VR): Used to visualize the spatial relationships of extracardiac

vessels and pulmonary and systemic venous drainage.

Multiplanar Reconstruction (MPR): This technique provided clear views of the lumen and vessel walls and was applied to all patients.

Maximum Intensity Projection (MIP): Highlighted vascular structures, particularly for assessing great vessels and pulmonary vein drainage.

Image interpretation: All images were evaluated by two independent radiologists using the segmental approach outlined by Lapierre et al. (7). Imaging analysis focused on supra-aortic arch branches and aorta from origin to bifurcation, assessing position, coarctation, interruption, and collateral branches. Pulmonary trunk and branches were evaluated for location, diameter, and branching collateral vessels and anomalies such as PAPVR, TAPVR, PDA, ASD, and VSD. The final diagnosis was established by correlating imaging findings with operative or cardiac catheterization data.

Cardiac catheterization was done for ten patients who underwent it for therapeutic purposes.

Statistical analysis:

Data analysis was conducted using SPSS software version 26 on a Windows 7 platform. Qualitative data were presented as absolute and relative frequencies, while quantitative data were expressed as mean and standard deviation (SD). The Chi-square test was applied for analyzing categorical variables, with a significance level set at $p < 0.05$. The Kappa statistics were used to evaluate the accuracy of the two methods by analyzing paired dependent qualitative data. The validity of TTE and MDCT in diagnosing anomalies was assessed through diagnostic performance measures based on 2x2 contingency tables, using catheterization or intraoperative findings as the reference (gold) standard. Sensitivity, specificity, positive predictive values (PPV), negative predictive values (NPV), and overall accuracy were calculated along with their 95% confidence intervals.

Inter-Rater Agreement: Agreement in anomaly detection between TTE, MDCT, and catheter/intraoperative findings was evaluated using the Chi-square test and Kappa statistics. The agreement was considered achieved if the Chi-square test result was insignificant and the Kappa statistic result was significant. The strength of the agreement was classified as follows:

K<0.2:Poor, K=0.21–0.40:Fair, K=0.41–0.60:Moderate, K=0.61–0.80:Good, K=0.81–1.00:Very good.

RESULTS

The study included 112 patients (60 females and 52 males) diagnosed clinically and by ECHO as having CHD and referred preoperatively to the MDCT unit. The mean age of the patients was 9.2±7.1 months. The patients were classified into three groups: the first group included patients with intra-cardiac malformations, the second group included patients with heart great vessel connection malformations, and the third group included patients with congenital vascular anomalies.

The common clinical presentations among the studied patients were dyspnea and cyanosis among 70% and 71.3%, respectively.

Regarding the cardiac malformations, they were represented in the following manner (Table 1): VSD (n=87;77,6%), RVOTO (n=52;46.4%), ASD (n=33;29.5%), PFO (n=13,6.25%), both single ventricle and dextrocardia each one represents (n=3; 2.6%), followed by a common atrium, juxtaposition of the atrial appendage, TV malformation, and double inlet ventricle each one of them represents (n=2; 1.7%), last one is MV malformation which is seen in one case; (0.9%). There was no significant difference between MDCT and ECHO in diagnosing cardiac structural malformations, except for the detection of PFO, where ECHO demonstrated greater accuracy ($p<0.05$) with a moderate Kappa agreement.

Regarding the heart-great vessels connection malformation shown in Table (2), there were 76 anomalies represented in the following frequencies:

TOF was seen in 49 cases (43.8%), followed by DORV in 19 cases (16.9%), TGA, and truncus arteriosus, each seen in 4 cases (3.6%). There was no significant difference between ECHO and MDCT in diagnosing heart-vascular connection malformations, with a good level of agreement reflected in the Kappa value. However, 3 cases with DORV were missed when assessed by ECHO. Table 3 demonstrates the congenital vascular anomalies; there were 175 anomalies.

Regarding the systemic thoracic arterial anomalies shown in table (3) seen as follows:

I. Aortic anomalies were detected in the form of Aortic arch anomalies seen in 26 cases (23%) which were represented in the following manner: right-sided aortic arch (21 cases), aberrant Rt SCA (5 cases), aberrant Lt SCA (4 cases), bovine aortic arch (3 cases), double aortic arch with hypoplastic left arch (1 case) and abnormal vertebral artery origin from the Aortic arch (1 case). The second common anomaly in this group is COA, which was diagnosed in 8 cases (7%), followed by bicuspid aortic valve seen in 6 cases (5.3%), followed by William syndrome and pseudo-coarctation each one was seen in 2 cases (1.8%), last one was diffused hypoplastic aorta which was seen in only one case (0.9%). This study demonstrated that MDCT discovered all these

aortic malformations, and a significant difference was observed between ECHO and MDCT in diagnosing most vascular structure malformations, particularly for aortic pseudo-coarctation (p = 0.04) and aortic arch anomalies (p = 0.02).

II. Coronary artery anomalies were diagnosed in 15 cases (13.4%). It was noticed that MDCT detected all coronary artery anomalies. In contrast, ECHO detected only 4% of cases as suspected of anomalous origin of LAD from RCA due to dilated RCA. This was augmented by the presence of a significant difference between MDCT and in diagnosing coronary artery anomalies (p=0.01).

III. Regarding Aortopulmonary connections seen in the form of PDA and MAPCAs. PDA was detected in 17 cases (15.2%), while MAPCAs were detected in 10 cases (9%). There was a significant difference between MDCT and ECHO in the diagnosis of PDA (p=0.04) and MAPCAs (p=0.01).

It is worth noting that the most significant p-value in the congenital vascular anomalies was for coronary artery anomalies and MAPCAs with poor agreement in kappa. Thus, the study demonstrated that MDCT is more accurate than ECHO in diagnosing these defects.

IV. Regarding pulmonary arteries, including: a) Supra valvular pulmonary stenosis was diagnosed in 35 cases (31.2%). MDCT successfully detected all cases, whereas ECHO missed 5 cases, showing a significant difference between MDCT and ECHO in diagnosing supravalvular pulmonary stenosis (p = 0.03). Conversely, pulmonary atresia was diagnosed in 10 cases (9%), with no difference between MDCT and ECHO.

V. Regarding the pulmonary venous anomalies, TAPVR was found in three cases (2.6%), while PAPVR in nine cases (8%).

VI. Systemic venous anomalies: In our study, various types of abnormal systemic venous drainage were observed, including PLSVC (18 cases, 16%), interrupted IVC, and retro-aortic left brachiocephalic vein, each detected in one case (0.9%). MDCT identified all these anomalies, whereas ECHO diagnosed only 11 cases (9.8%), showing a significant difference between MDCT and ECHO in the detection of systemic venous anomalies. In contrast, there was no significant difference between MDCT and ECHO in diagnosing other vascular defects, such as aortic coarctation, pulmonary atresia, or abnormal pulmonary venous drainage.

Table 4 shows the results of the agreement between catheter/ intraoperative, MDCT, and ECHO in diagnosing CHD. There was a very good level of agreement between each of ECHO and MDCT and catheter/surgery in the detection of the intra-cardiac structures' malformations with kappa =1.000 and kappa = 0.890, respectively. The strength of agreement in the evaluation of the heart–vascular connection malformation was very good for both MDCT and ECHO compared to cardiac catheter/surgery with k=1.0000 and 0.919 respectively, SE = 0.000 and 0.039, respectively, and 95% CI was 1.000 and 0.945 respectively. The strength of agreement diminished when assessing thoracic vascular anomalies. However, the agreement between MDCT and cardiac catheterization/surgery remained very good (k=1.000), the agreement between ECHO and cardiac catheterization /surgery was moderate (k=0.80), with standard errors of 0.000 and 0.066, respectively, and 95% confidence intervals of 1.000 and 0.937, respectively. Additionally, the agreement and significance between TTE and MDCT were measured. There was very good agreement (k=0.890) in the detection of cardiac structural malformations. For heart–vascular connection malformations, the agreement was also very good (k = 0.919). However, for congenital vascular anomalies, the agreement was moderate (k = 0.80), with standard errors of 0.076, 0.039, and 0.066, respectively.

Table 5 shows the specificity, sensitivity, positive and negative predictive values, and accuracy of ECHO & MDCT in diagnosing CHD: It was noticed that both ECHO and MDCT were nearly similar in sensitivity and specificity in diagnosing cardiac malformations. However, MDCT showed better sensitivity, accuracy, and NPV value in diagnosing each heart vascular connection malformations and congenital vascular anomalies. Sensitivity, specificity, and accuracy were (93%, 100%, and 95%) for ECHO in the diagnosis of congenital vascular anomalies and was (100 %, 100%, and 100 %) for MDCT, respectively. The associated pulmonary lesions among the studied cases were resolving consolidation was detected in 36 cases (32%), atelectasis in 8 cases (7 %), and 2 cases of TOF with hypoplastic left lung. All were detected only by MDCTA.

Tables:

Table 1: Comparison between ECHO and MDCT in the diagnosis of intra-cardiac malformation identified by surgery.

tra-Cardiac structure malformation	ırgery	DCT TP	DCT TN	DCT FP	DCT FN	CHO TP	CHO TN	CHO FP	CHO FN	value	ppa
VSD	87	87	25	0	0	85	25	0	2	0.06	799
Secundum ASD	23	20	89	0	3	23	89	0	0	0.07	763
PFO	13	8	99	0	5	13	99	0	0	**0.04**	732
SSVASD	5	5	107	0	0	5	.07	0	0	0.1	987
-roofed coronary sinus	2	2	110	0	0	2	0	0	0	0.9	981
Primum ASD	3	3	109	0	0	3	.09	0	0	0.09	894
CAVC	6	6	105	0	0	7	.05	0	0	1	991
Dextrocardia	3	3	109	0	0	3	.09	0	0	1	981
RVOTO	52	52	60	0	0	52	60	0	0	0.9	911
Common atrium	2	2	110	0	0	2	.10	0	0	0.4	902
Single ventricle	3	3	109	0	0	3	.09	0	0	0.7	911
TV malformation	3	2	110	0	1	3	.09	0	0	0.3	799
MV malformation	1	1	111	0	0	1	.11	0	0	1	981
juxtaposition of atrial appendage	2	2	110	0	0	2	.10	0	0	0.9	981
ouble inlet ventricle	2	2	110	0	0	2	.10	0	0	0.9	981
Total	207										

**True positive (TP), true negative (TN), false positive (FP), false negative (FN).

Table 2: Comparison between ECHO and MDCT in diagnosis of heart -great vessel connection malformation identified by surgery

Heart-vascular connection	Surgery	DCT TP	DCT TN	DCT FP	DCT FN	HO TP	HO TN	HO FP	HO FN	p-value	Kappa
TOF	49	49	63	0	0	49	63	0	0	0.7	0.93
DORV	19	19	93	0	0	16	90	0	3	0.08	0.75
TGA	4	4	108	0	0	3	108	0	1	0.9	0.85
TRUNCUS ARTERIOSUS	4	4	108	0	0	4	108	0	0	0.9	0.96
Total	76										

**True positive (TP), true negative (TN), false positive (FP), false negative (FN).

Table (3) Comparison between MDCT and ECHO in the diagnosis of congenital vascular anomalies:

scular malformation	ath/ gery	DCT TP	DCT TN	DCT FP	DCT FN	HO TP	HO TN	HO FP	HO FN	lue	pa
CoA	8	8	104	0	0	7	104	0	1	09	6
PSEUDO-CoA	2	2	110	0	0	0	110	0	2	**04**	9
rtic arch anomalies	26	26	89	0	0	13	89	0	13	**02**	4
cuspid aortic valve	6	6	106	0	0	6	106	0	0	9	9
William syndrome	2	2	110	0	0	1	110	0	1	07	12
use hypoplastic aorta	1	1	111	0	0	1	111	0	0	05	0
avalvular pulmonary stenosis	35	35	77	0	0	30	77	0	5	**03**	8
Pulmonary atresia	10	10	102	0	0	8	102	0	2	08	86
PDA	17	17	95	0	0	12	95	0	5	**04**	15
Coronary Artery Anomalies	15	15	97	0	0	5	97	0	10	**01**	47
MAPCAs	10	10	102	0	0	2	102	0	8	**01**	39

PAPVR	9	9	103	0	0	8	103	0	1	8	3
TAPVR	3	3	109	0	0	2	109	0	1	9	9
LT SVC	18	18	94	0	0	11	94	0	7	**03**	16
ETROAORTIC BCV	1	1	111	0	0	0	111	0	1	06	8
Interrupted IVC with azygos continuation	1	1	111	0	0	0	111	0	1	06	8
Total	175										

**True positive (TP), true negative (TN), false positive (FP), false negative (FN).

Table 4: The agreement between catheter/intraoperative, ECHO, and MDCT in the diagnosis of CHD:

Findings	Kappa	SE	95% CI
1- Cardiac malformations:			
a) ECHO & cath/surgery	1.000	0.00	1.000
b) MDCT & Cath/intraoperative	0.890	0.076	0.974-1.000
c) ECHO & MDCT	0.890	0.076	0.974-1.000
2- Heart-vascular connection malformation:			
a) ECHO & Cath/surgery	0.919	0.039	0.945
b) MDCT & Cath/intraoperative	1.000	0.000	1.000
c) ECHO & MDCT	0.919	0.039	0.940
3- Congenital vascular anomalies			
a) ECHO & Cath/surgery	0.80	0.066	0.937
b) MDCT & Cath/intraoperative	1.000	0.000	1.000
c) ECHO & MDCT	0.80	0.066	0.937

Table 5: Sensitivity, specificity, positive and negative predictive values and accuracy of ECHO & MDCT in diagnosis of CHD identified by cath/intraoperative findings:

Findings	nsitivity	ecificity	ccuracy	PPV	NPV	AUC
Cardiac malformations:						
a) ECHO	99%	100%	99%	100%	90%	1.000
b) MDCT	98%	100%	98%	100%	89%	0.990
Heart -vascular connection:						
a) ECHO	95%	100%	96%	100%	90%	0.974
b) MDCT	99%	100%	99%	100%	98%	1.000
Thoracic vascular malformation:						
a) ECHO	93%	100%	95%	100%	76%	0.80
b) MDCT	100%	100%	100%	100%	100%	1.000

Positive predictive value (PPV), negative predictive value (NPV), area under the curve (AUC).

Figures

a) 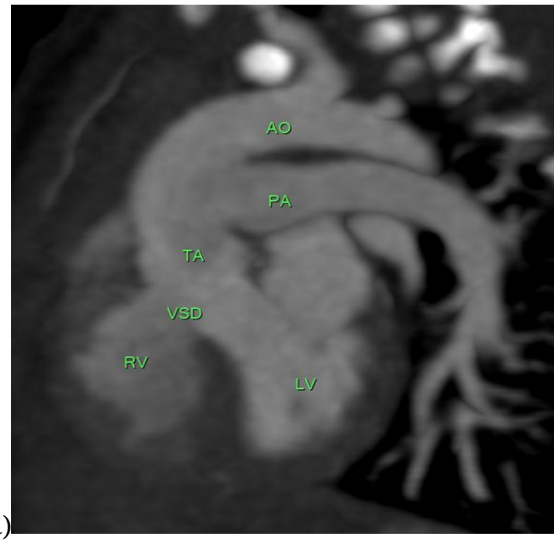

b) 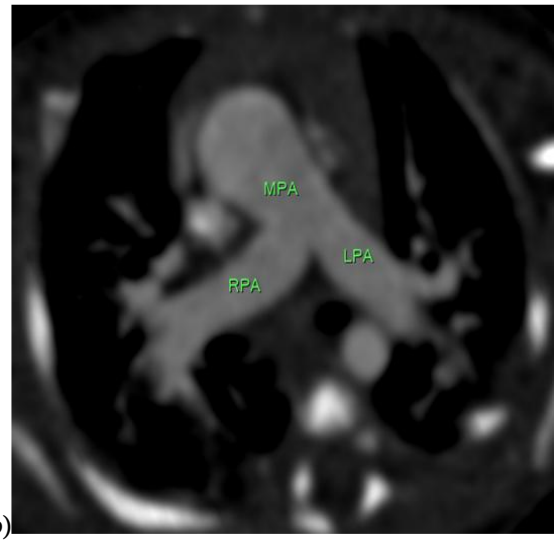

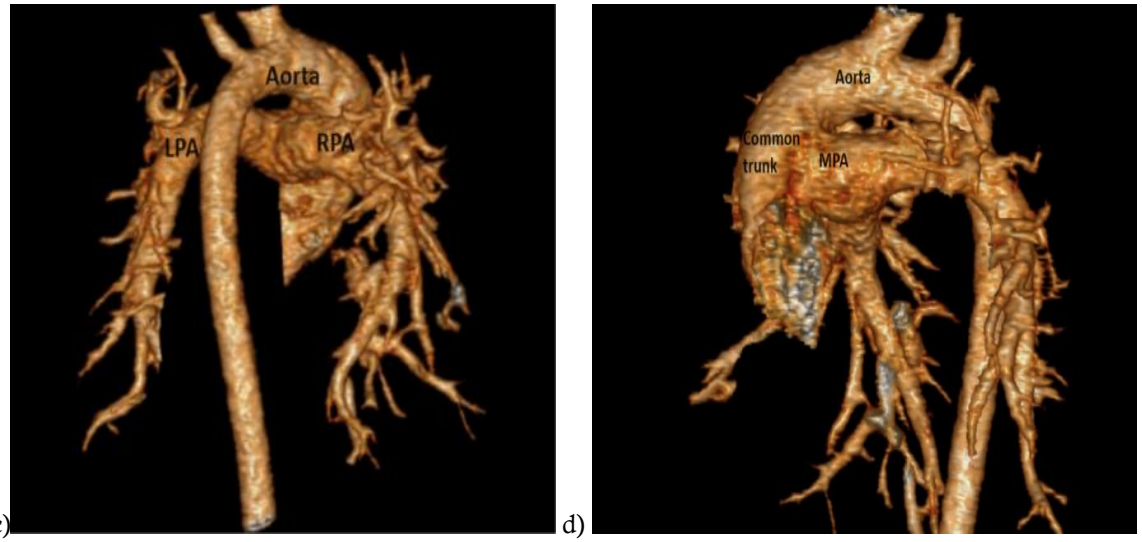

c) d)

Figure 1: A case of truncus arteriosus type I in an infant one-month-old, reformatted short axis view and axial view (1.a&b) shows common arterial trunk overriding both ventricles through conoventricular VSD, the common trunk supplies both the aorta and the short pulmonary trunk, which subsequently divides into the right and left pulmonary arteries. A 3D VR image (posterior view, 1.c) illustrates the common arterial trunk branching into the aorta and pulmonary artery, with the right and left pulmonary arteries arising posteriorly. Another 3D VR image (anterior oblique view, 1.d) demonstrates the main pulmonary artery (MPA) originating from the posterior aspect of the common arterial trunk.

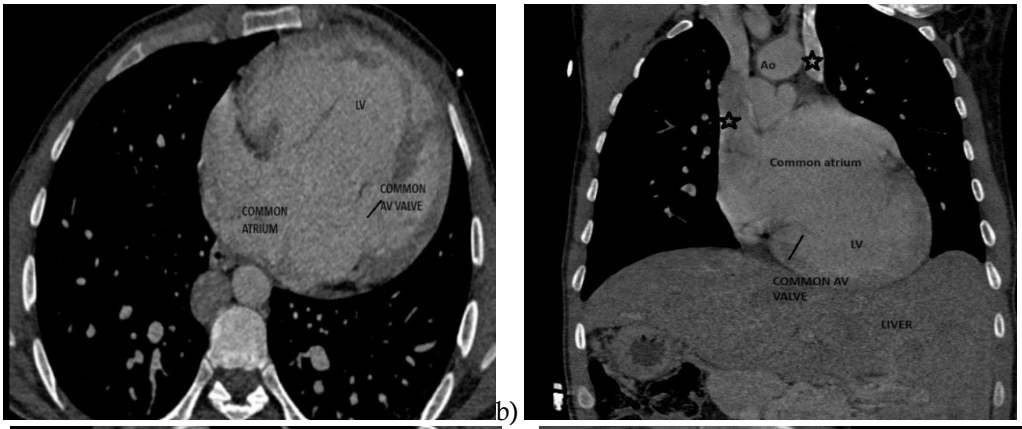

b)

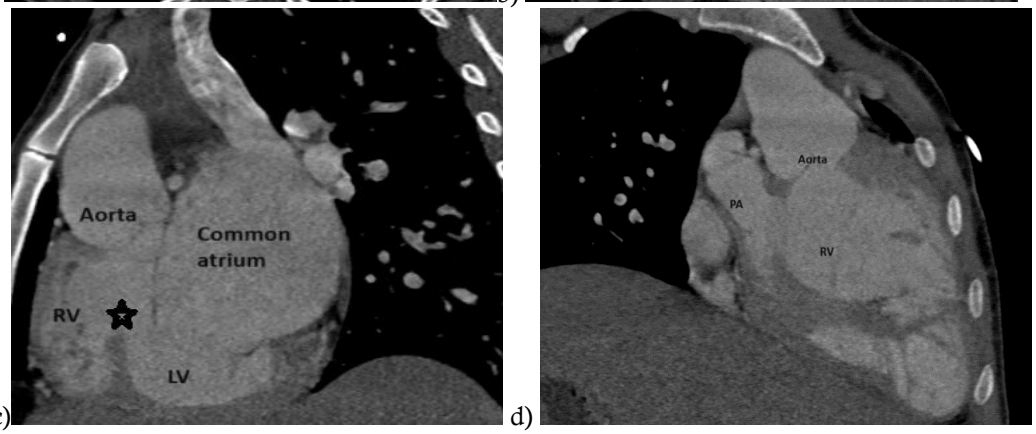

c) d)

e) 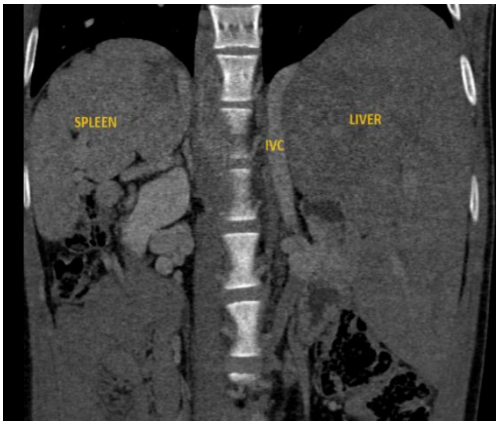

f) 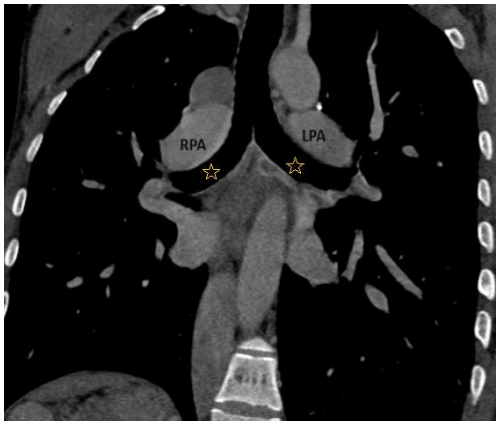

Figure 2 demonstrates a case of situs inversus with left isomerism and interrupted IVC with azygos continuation, DORV. Reformatted MDCT is axial (2.a) and coronal (2.b) view shows common atrium, common AV valve with five leaflets with the dilated left ventricle, also note (black stars) on the right and left SVC, both drain in the common atrium. note situs inversus in the form of liver on the left side, stomach, and spleen on the right side. Reformatted two-chamber view (2.c) shows the right ventricle and left ventricle with large outlet VSD with inlet extension (black star). Reformatted coronal oblique view (2.d) shows DORV, Reformatted MDCT coronal view (2.e) shows situs inversus of the abdominal viscera as liver on the left side and spleen on the right side with polysplenia, also left-sided interrupted IVC is noted. Reformatted MDCT coronal view (2.f) shows bilateral hyparterial bronchi with left morphology.

Figure: 3 Tricuspid atresia with hypoplastic RV, Secondum ASD with small outlet VSD

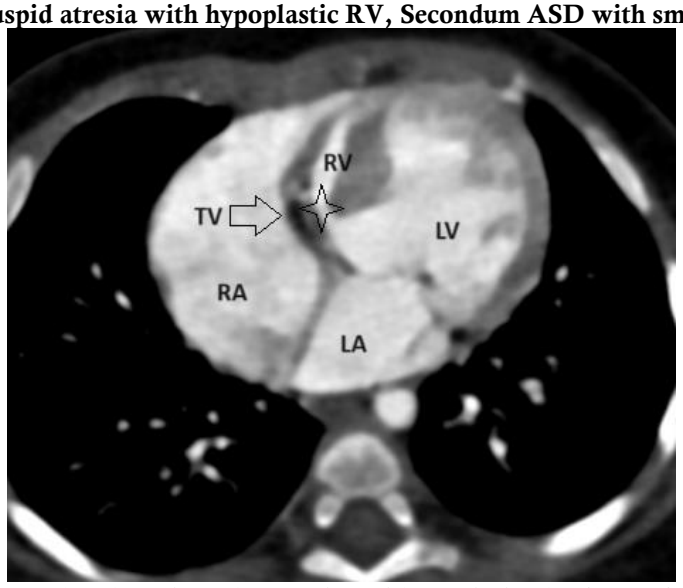

(A) Reformatted MDCT four-chamber view shows tricuspid atresia in the form of replacement of the normal valve leaflet by fibro-fatty tissue, associated with hypoplastic right ventricle with small VSD (asterisk), dilated right atrium, dilated left ventricle.

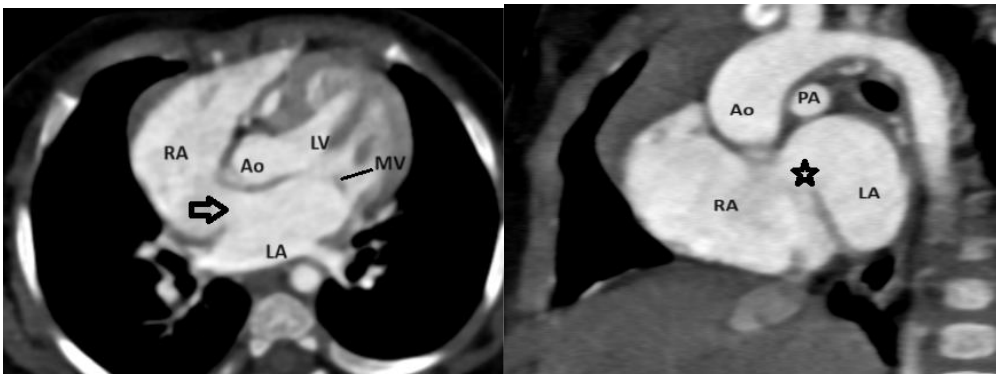

(B, C) Reformatted MDCT four-chamber view and sagittal view shows secondum ASD.

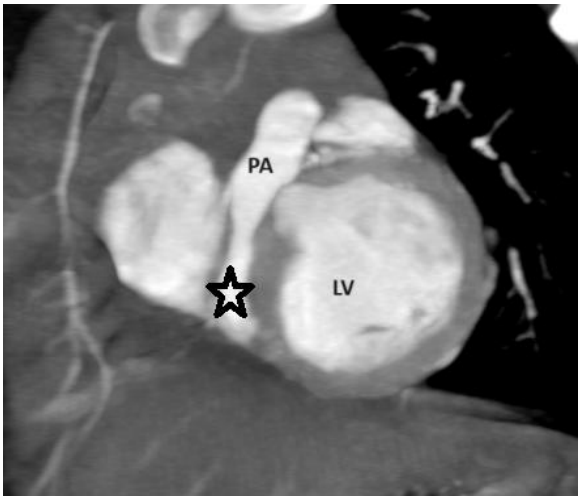

(D) Reformatted MDCT two-chamber view (D) shows hypoplastic RV with average-sized pulmonary artery arising from the RV,

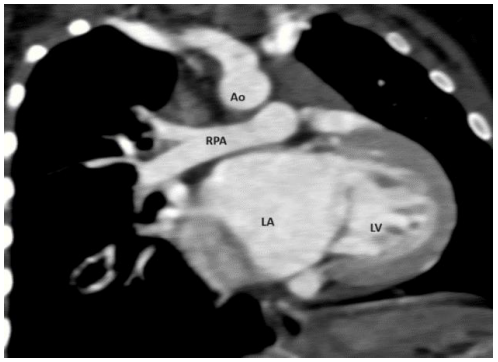

(E) MDCT coronal view (E) shows RPA with average size,

DISCUSSION

Accurate and thorough preoperative evaluation of complex CHD is essential for selecting the suitable surgical technique and assessing prognosis. Advances in surgical and medical care for CHD patients have significantly improved survival rates, even for the most complex conditions. Additionally, patients with operated CHD need periodic diagnostic evaluations throughout their lives (Marelli et al., (8). ECHO remains the primary diagnostic tool for CHD due to its noninvasive nature, rapidity, affordability, and wide availability, reducing the reliance on diagnostic cardiac catheterization and angiography (Saad et al., (9)). Meanwhile, enhanced resolution, fast image acquisition, and reduced radiation exposure of modern CT machines have greatly expanded the MDCT role in evaluating CHD patients across all age groups, particularly in pediatrics (Bu et al., (10).

MDCT has proven valuable in categorizing pulmonary situs, particularly in demonstrating the eparterial or hyparterial positions of bronchi in cases of heterotaxy syndrome, visceral malposition, asplenia, and polysplenia (Shehata et al., (11). Moreover, MDCT has a greater value in providing an accurate anatomical assessment of RVOT, coronary, and pulmonary artery anomalies, which is crucial for imaging complex CHD (Saad et al., (9).

In this study, complex CHD accounted for approximately half of our cohort. Regarding the diagnosis of intra-cardiac structural malformations, the results showed no significant difference between ECHO and MDCT, with a KAPPA of 0.890 and a p-value >0.05. The accuracy was 99% for ECHO and 98% for MDCT, indicating that both modalities have comparable accuracy in detecting intracardiac anomalies. However, a significant difference was observed in the diagnosis of PFO, where ECHO was more precise than MDCT.

Our findings align with those of Öztürk et al. (12), who reported that ECHO was more accurate than CTA in identifying intracardiac malformations. Similarly, our results are consistent with Saad et al. (9), who found that the sensitivity of ECHO was 100% and MDCT was 92.9%, with a significant difference favoring ECHO in the diagnosis of PFO. Similar results were proved by Harvey et al. (13) and Aiyin et al. (14).

In this study, the assessment of atrioventricular valves revealed one case of a dysplastic tricuspid valve and one case of tricuspid regurgitation, both accurately diagnosed by ECHO but not precisely identified by MDCT. This discrepancy is attributed to the limitations of MDCT's static images, which are unable to provide detailed information on

hemodynamic variations and valvular structures. On the other hand, ECHO's dynamic imaging capabilities allow for the detection of shunts, regurgitation, and intracardiac structures (Öztürk et al., (12).

Regarding VSD, there was no significant difference between the two tools of investigation. However, ECHO missed three cases of VSDs, one of which was diagnosed by echocardiography as two small VSDs. However, MDCT detected multiple muscular and apical VSDs (Swiss-cheese VSD), which leads to a different opinion about the patient's management, as Swiss-cheese VSD is managed as univentricular repair, not biventricular repair.

In this study, no significant difference was observed between MDCT and ECHO in diagnosing malformations of heart-vascular connections. The sensitivity was 95% and 99%, specificity was 100% for both, and accuracy was 96% and 99%, respectively, indicating that both modalities could effectively and accurately diagnose these malformations. These findings are consistent with the results of Saad et al. (9) and Aiyin et al. (14).

However, Echo missed three cases of DORV. It diagnosed them as TOF, which included the following cases: The first case was a female patient, four years old, diagnosed by Echo as TOF and diagnosed by MDCT as DORV with inlet or remote VSD. The second case was a two-month-old male patient diagnosed by Echo as TOF, on MDCT, diagnosed as DORV Fallot type with subvalvular and valvular pulmonary stenosis with additional mid-muscular and apical VSDs. Differentiating between the two conditions is crucial for surgical repair. Among our cases was a male patient. Echo diagnosed him with truncus arteriosus with inlet VSD. MDCT detected a DORV anomaly with perimembranous VSD and a double aortic arch with a hypoplastic left arch. The MDCT findings totally agreed with the operative data.

The last case was a male patient diagnosed by Echo as DORV with pulmonary stenosis, perimembranous VSD, and TAPVR (supracardiac type). MDCT found that the patient had a DORV anomaly with pulmonary stenosis and subaortic VSD, normal pulmonary venous drainage (all pulmonary veins drain to the left atrium), which totally agrees with the intra-operative data.

In the current study, a significant difference was observed in the diagnostic accuracy of MDCT and ECHO for vascular malformations, where the accuracy of ECHO was 95% and 100% for MDCT, with KAPPA= 0.80 for ECHO vs. 1 for MDCT, sensitivity, and specificity were 93% and 100% for ECHO and 100% for MDCT. The previous results were in line with Aiyin et al. (14), who found that the diagnostic accuracy of MSCT and ECHO were 98.30% and 96.30%, respectively. The same results were recorded by (Saad et al. (9). Our results were in contrast with Öztürk et al. (12), who showed that there was no significant difference in predicting great vessel malformations between the two methods.

Regarding Aortic anomalies, MDCT angiography has recently emerged as the primary diagnostic tool for assessing thoracic aortic anomalies. It serves as a replacement for cardiac catheterization in evaluating aortic diseases, particularly in cases where catheterization is not feasible for arch obstructive anomalies (Kimura-Hayama et al., (15)). Additionally, MDCT can complement echocardiography by providing detailed visualization of anomalous arch configurations and branching patterns, which is critical for surgical planning in conditions such as truncus arteriosus and TGA.

In the current study, arch obstructive anomalies (coarctation) were observed among the cases. MDCT effectively identified the type, specific location, extent, degree of stenosis, and the distance between the proximal and distal aortic segments and the formation of collateral vessels in these lesions. Our findings are in line with previous reports conducted by Dillman and Hernandez (16), Long et al. (17), Al-Azzazy et al. (18), and Shehata et al. (11).

A previous study (Long et al. 17) showed that MDCT is an excellent modality for evaluating suspected vascular rings and slings, as it effectively demonstrates the anatomical connection between the vascular structures and trachea, which aligns with this study. We identified various types of aortic arch anomalies in 24 cases. All anomalies were detected using MDCT, whereas ECHO missed 8 of these cases.

In the current study, our findings demonstrated that MDCT successfully identified five cases of left aortic arch with an aberrant right subclavian artery (ARSCA), four cases of right aortic arch with an aberrant left subclavian artery, and one case of double aortic arch with a hypoplastic left arch. MDCT also allowed for the determination of the dominant right arch and provided a clear depiction of the relationship between each arch, the great vessels, and the airway.

Consistent with the findings of Adaletli et al. (19) and Saad et al. (9), our study revealed a significant difference between MDCT and ECHO in evaluating aortic arch anomalies ($p<0.05$). MDCT proved to be significantly superior to ECHO in diagnosing the aortic arch anomalies observed in this study.

Our findings on RVOT and pulmonary artery

anomalies demonstrated that MDCT can accurately diagnose RVOT abnormalities, anomalous origins of pulmonary arteries, and various congenital pulmonary artery anomalies with proximal interruption, agenesis, stenosis, and aortopulmonary collateral flow. These anomalies can occur either in isolation or in association with other congenital heart diseases. In this study, there was a significant difference between ECHO and MDCT in diagnosing pulmonary arterial anomalies and aortopulmonary collaterals in patients with severe right ventricular outflow tract obstruction or pulmonary atresia. These findings are consistent with those of Sigal-Cinqualbre et al. (20), Abd El-Gaber and Alsawah (21), Ahmed et al. (22), Shehata et al. (11), and Saad et al. (9), who reported a significant difference between ECHO and MDCT in diagnosing supravalvular pulmonary stenosis and MAPCAs, with $p<0.05$ in these cases. This underscores that MDCT is superior to ECHO in diagnosing these anomalies, playing a critical role in preoperative and/or catheterization planning.

Regarding PDA, Aiyin et al. (14) stated that TTE is the preferred modality for diagnosing patent ductus arteriosus. However, MDCT offers additional advantages by providing detailed visualization of ductal size, morphology, and calcifications, which are crucial factors for treatment (Leschka et al., (23)). In this study, a significant difference was observed between MDCT and ECHO in diagnosing PDA, demonstrating that MDCT was superior to TTE for this purpose. These findings are consistent with the results reported by Shehata et al. (11). Still in contrast to Leschka et al. (23). This controversy in the diagnostic accuracy of ECHO in detection of PDA could be attributed to diagnostic error of echocardiography in detection of PDA, especially in cases with pulmonary hypertension or increase follow of pulmonary artery as in these cases the low flow between aorta and pulmonary artery occurs due to equalization of the pressure between aorta and pulmonary artery.

Regarding the systemic and pulmonary venous return:

MDCT allowed for precise delineation of veno-atrial connections. Systemic venous anomalies identified included a persistent left superior vena cava (LT SVC) in 18 cases (16%), a retro-aortic left brachiocephalic vein in 1 case (0.9%), and an interrupted inferior vena cava (IVC) in 1 case (0.9%). MDCT exclusively detected both the retro-aortic brachiocephalic vein and the interrupted IVC. A significant difference was observed between MDCT and ECHO in detecting LT SVC ($p = 0.03$). The diagnostic limitations of echocardiography in identifying extracardiac structures, such as a persistent left SVC, may stem from the similar echodensities of these structures and the absence of coronary sinus dilation, which can otherwise suggest anomalous systemic venous drainage.

Additionally, MDCT accurately depicted normal pulmonary venous return into the left atrium in all cases. MDCT proved superior to ECHO in assessing systemic venous anomalies. The sensitivity, specificity, accuracy, positive predictive value (+PV), and negative predictive value (-PV) for TTE and MDCT in detecting systemic venous anomalies were as follows:

TTE: 83.3%, 98.2%, 98%, 100%, and 98%, respectively.

MDCT:100%, 100%, 100%, and 100%, respectively.

Conclusion: This study revealed that the main added value of MDCTA to echocardiography is better and more accurate diagnoses of extracardiac vascular anatomic structures, which could replace the need for invasive catheterization, especially in children.

Abbreviations:

3DVR: Three-dimensional volume rendering
ARSCA: Aberrant right subclavian artery
ASD: Atrial septal defect
CAVC: Common atrioventricular canal
CHD: Congenital heart disease
CoA: Coarctation of aorta
CTA: Computed tomography angiography
DORV: Double outlet right ventricle
IVC: Inferior vena cava
LV: Left ventricle
MAPCAS: Multiple aortopulmonary collaterals
MDCT: Multidetector computed tomography
MIP: Maximal intensity projection
MPR: Multiplanar reconstruction
PA: Pulmonary artery
PAPVR: Partial anomalous pulmonary venous return
PDA: Patent ductus arteriosus
PFO: Patent foramen ovale
RV: Right ventricle
SCA: Subclavian artery
SVC: Superior vena cava
TAPVR: Total anomalous pulmonary venous return
TGA: Transposition of great arteries
TOF: Tetralogy of Fallot
VSD: Ventricular septal defect

References

1. Madsen NL, Marino BS, Woo JG, Thomsen RW, Videbøk J, Laursen HB, et al. Congenital heart disease with and without cyanotic potential and the long-term risk of diabetes mellitus: a population-based follow-up study. J Am Heart Assoc. 2016;5(7):e003076.
2. Khatri S, Varma SK, Khatri P, Kumar RS. 64-slice multidetector-row computed tomographic angiography for evaluating congenital heart disease. Pediatr Cardiol. 2008;29:755-762.
3. Rao PS. Diagnosis and management of cyanotic congenital heart disease: Part II. Indian J

Pediatr. 2009;76:297-308.
4. Paul JF, Rohnean A, Sigal-Cinqualbre A. Multidetector CT for congenital heart patients: what a paediatric radiologist should know. Pediatr Radiol. 2010;40:869-875.
5. Goitein Y, Salem Y, Jacobson J, et al. The role of cardiac computed tomography in infants with congenital heart disease. Isr Med Assoc J. 2014;16(3):147-152.
6. Hellinger JC, Daubert M, Lee EY, Epelman M. Congenital thoracic vascular anomalies: evaluation with state-of-the-art MR imaging and MDCT. Radiol Clin. 2011;49(5):969-996.
7. Lapierre C, Déry J, Guérin R, Viremouneix L, Dubois J, Garel L. Segmental approach to imaging of congenital heart disease. Radiographics. 2010;30(2):397-411.
8. Marelli AJ, Ionescu-Ittu R, Mackie AS, Guo L, Dendukuri N, Kaouache M. Lifetime prevalence of congenital heart disease in the general population from 2000 to 2010. Circulation. 2014;130(9):749-756.
9. Saad MA, Abdel Halim AM, Abo Elnour SI, Abbas AFaA. Role of Cardiac CT in evaluating vascular versus cardiac congenital heart diseases in children. Med J Cairo Univ. 2021;89(Dec):2617-2631.
10. Bu G, Miao Y, Bin J, Deng S, Liu T, Jiang H, et al. Comparison of 128-slice low-dose prospective ECG-gated CT scanning and trans-thoracic echocardiography for the diagnosis of complex congenital heart disease. PLoS One. 2016;11(10):e0165617.
11. Shehata S, Zaiton F, Warda MA, Shahbah D, Ebrahim B. Value of MDCT as a noninvasive modality in evaluation of pediatric congenital cardiovascular anomalies. Egypt J Radiol Nucl Med. 2017;48(2):467-478.
12. Öztürk E, Tanıdır IC, Kamalı H, Ayyıldız P, Topel C, Onan İS, et al. Comparison of echocardiography and 320-row multidetector computed tomography for the diagnosis of congenital heart disease in children. Rev Port Cardiol (Engl Ed). 2021;40(8):583-590.
13. Harvey J, Hoey E, Ganeshan A. Imaging of the aortic valve with MRI and CT angiography. Clin Radiol. 2013;68(12):1192-1205.
14. Aiyin L, Peng Z, Zhang C. Comparison of echocardiography and 64-multislice spiral computed tomography for the diagnosis of pediatric congenital heart disease. Med Sci Monit. 2017;23:2258.
15. Kimura-Hayama ET, Meléndez G, Mendizábal AL, Meave-González A, Zambrana GFB, Corona-Villalobos CP. Uncommon congenital and acquired aortic diseases: role of multidetector CT angiography. Radiographics. 2010;30(1):79-98.
16. Dillman JR, Hernandez RJ. Role of CT in the evaluation of congenital cardiovascular disease in children. AJR Am J Roentgenol. 2009;192(5):1219-1231.
17. Long YG, Yang YY, Huang IL, Pan JY, Wu MT, Weng KP, et al. Role of multislice and three-dimensional computed tomography in delineating extracardiac vascular abnormalities in neonates. Pediatr Neonatol. 2010;51(4):227-234.
18. Al-Azzazy MZ, Nasr MS, Shoura MA. Multidetector computed tomography (MDCT) angiography of thoracic aortic coarctation in pediatric patients: preoperative evaluation. Egypt J Radiol Nucl Med. 2014;45(1):159-167.
19. Adaletli İ, Barış S, Kılıç F, Özdil M, Güzeltaş A, Demir T, et al. Multislice computed tomography angiography is a sufficient method for detecting native aortic coarctation in children. Turk J Thorac Cardiovasc Surg. 2011;19(3).
20. Sigal-Cinqualbre A, Lambert V, Rohnean A, Paul J. Role of MSCT and MRI in the diagnosis of congenital heart disease. Arch Pediatr. 2011;18(5):617-627.
21. Abd El-Gaber N, Alsawah GA. Role of 16-multidetector CT angiography in assessment of arterial and venous pulmonary anomalies in pediatrics. Egypt J Radiol Nucl Med. 2013;44(3):483-495.
22. Ahmed AEM, Mohamed YG, Amin SA, Elfakhrany SN. The role of multislice computerized tomography (MSCT) in evaluation of complex congenital heart diseases in pediatric patients. Egypt J Pediatr. 2016;33(1):143-153.
23. Leschka S, Oechslin E, Husmann L, Desbiolles L, Marincek B, Genoni M, et al. Pre- and postoperative evaluation of congenital heart disease in children and adults with 64-section CT. Radiographics. 2007;27(3):829-846.
24. Mccollough CH, Primak AN, Braun N, Kofler J, Yu L, Christner J. Strategies for reducing radiation dose in CT. Radiol Clin. 2009;47(1):27-40.
25. Park M. Complete transposition of the great arteries. In: The Pediatric Cardiology Handbook. 4th ed. Philadelphia, PA: Mosby Elsevier; 2010:120-128.
26. Thomas KE, Wang B. Age-specific effective doses for pediatric MSCT examinations at a large children's hospital using DLP conversion coefficients: a simple estimation method. Pediatr Radiol. 2008;38:645-656.

